

## Photophysical Studies of the Trans to Cis Isomerization of the Push–Pull Molecule: 1-(Pyridin-4-yl)-2-(*N*-methylpyrrol-2-yl)ethene (mepepy)

Audrey Mokdad, Jonathan L. Belof, Sung Wook Yi, Stephen E. Shuler, Mark L. McLaughlin, Brian Space, and Randy W. Larsen\*<sup>†</sup>

Department of Chemistry, University of South Florida, 4202 E. Fowler Avenue, Tampa, Florida 33620

Received: April 15, 2008; Revised Manuscript Received: June 20, 2008

Organic molecules possessing intramolecular charge-transfer properties ( $D-\pi-A$  type molecules) are of key interest particularly in the development of new optoelectronic materials as well as photoinduced magnetism. One such class of  $D-\pi-A$  molecules that is of particular interest contains photoswitchable intramolecular charge-transfer states via a photoisomerizable  $\pi$ -system linking the donor and acceptor groups. Here we report the photophysical and electronic properties of the trans to cis isomerization of 1-(pyridin-4-yl)-2-(*N*-methylpyrrol-2-yl)ethene ligand (mepepy) in aqueous solution using photoacoustic calorimetry (PAC) and theoretical methods. Density functional theory (DFT) calculations demonstrate a global energy difference between cis and trans isomers of mepepy to be 8 kcal mol<sup>-1</sup>, while a slightly lower energy is observed between the local minima for the trans and cis isomers (7 kcal mol<sup>-1</sup>). Interestingly, the trans isomer appears to exhibit two ground-state minima separated by an energy barrier of  $\sim 9$  kcal mol<sup>-1</sup>. Results from the PAC studies indicate that the trans to cis isomerization results in a negligible volume change ( $0.9 \pm 0.4$  mL mol<sup>-1</sup>) and an enthalpy change of  $18 \pm 3$  kcal mol<sup>-1</sup>. The fact that the acoustic waves associated with the trans to cis transition of mepepy overlap in frequency with those of a calorimetric reference implies that the conformational transition occurs faster than the  $\sim 50$  ns response time of the acoustic detector. Comparison of the experimental results with theoretical studies provide evidence for a mechanism in which the trans to cis isomerization of mepepy results in the loss of a hydrogen bond between a water molecule and the pyridine ring of mepepy.

### Introduction

The importance of nonlinear optical materials in high-speed optical modulators, optical storage media, and fast/ultrafast optical switches, etc., has stimulated research efforts into the development and characterization of novel classes of molecules which can exhibit diverse polarization properties both in the ground and excited states.<sup>1–5</sup> One class of molecules which have demonstrated nonlinear optical (NLO) properties and are of current research interest is known as “push–pull” type molecules. The nonlinear optical effects associated with these molecules are due to the presence of an electron-accepting group on one side of a conjugated moiety and an electron-donating group on the opposite side. This enhances the polarizability of the double bond region allowing for additional polarization to be induced in the presence of an electric field. Typically, amino, dialkylamino, ether, or oxide (O<sup>-</sup>) functional groups form the electron-donating substituent while nitro, carbonyl, and cyano groups are employed as the corresponding acceptor group.<sup>6,7</sup> To achieve the desired polarizability, these groups are separated via a conjugated linker group.

In addition to their nonlinear optical properties, push–pull molecules have also been utilized as ligands for various transition metal complexes in order to photolytically alter the spin state of the complex.<sup>8–13</sup> In this case the push–pull ligand must possess a functional group capable of coordinating to the transition metal complex and that exhibits a shift in the basicity upon photoexcitation. Metal complexes of this type can exhibit,

for example, a low-spin electron configuration when the push–pull ligand is in the more basic conformation and switch to a high-spin configuration upon photoconversion of the ligand to the less basic conformation. A number of such complexes have now been synthesized and their optical and magnetic properties examined. These include complexes of the Fe<sup>II</sup>(L<sub>4</sub>)-(X<sub>2</sub>) type in which L is the photoisomerizable push–pull ligand and of the Fe<sup>III</sup>(L<sub>4</sub>)(L')(X) type in which L' is the push–pull ligand. Early studies utilized 4-sterylpyridine (Stpy; 1-phenyl-2-(4-pyridyl)ethane) as well as several phenyl derivatives of this ligand to photoinduce the spin crossover.<sup>10–12</sup> In one of the first examples of ligand-driven, light-induced spin-state changes, the Fe<sup>II</sup>(*trans*-Stpy)<sub>4</sub>(NCS)<sub>2</sub> complex was found to undergo a thermally induced high-spin to low-spin transition centered near 190 K.<sup>10</sup> Photoexcitation of this complex imbedded within a cellulose acetate substrate at 140 K results in trans to cis isomerization of the Stpy, which also induces the high-spin to low-spin transition.

The success of these complexes has led to the synthesis of new compounds which exhibit ligand-driven, light-induced spin-state changes at higher temperatures. One such complex, [Fe<sup>III</sup>(salten)(mepepy)]BPh<sub>4</sub> (salten = 4-azaheptamethylene-1,7-bis(salicylideneimine)); mepepy = 1-(pyridin-4-yl)-2-(*N*-methylpyrrol-2-yl)ethene; BPh<sub>4</sub> = tetraphenyl borate) has been shown to exhibit a high-spin to low-spin transition at room temperature under visible irradiation.<sup>11–13</sup> Unlike the Fe<sup>II</sup>(L<sub>4</sub>)-(X<sub>2</sub>) type complexes discussed above, which have four photoisomerizable ligands, the Fe<sup>III</sup>(L<sub>4</sub>)(L')(X) type complexes (e.g., Fe<sup>III</sup>(salten)(mepepy)) have only a single isomerizable ligand which is used to modulate the ligand field strength. In the case

\* To whom correspondence should be addressed. E-mail: rlarsen@cas.usf.edu.

<sup>†</sup> Contributed from USF-SMMARIT (Center for Smart Metal Organic Materials Advanced Research and Technology Transfer).

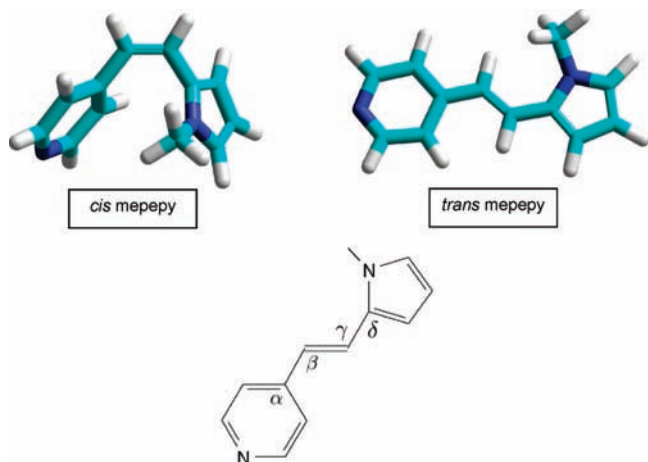


**Figure 1.** Structural diagrams of the trans and cis conformations of mepepy.

of the mepepy complex the spin-state transition is triggered via the light-induced trans to cis isomerization of the ligand, which results in a shift in electron density from the *N*-methylpyrrole moiety to the pyridine unit (see Figure 1 for a structural diagram of mepepy).

Although the trans/cis photoisomerization of mepepy has been shown to be effective in modulating the ligand field strength of the chromophore, much less is known about the electron properties and energetics of this process. The optical spectrum of the trans conformation of mepepy in acetonitrile exhibits absorption maxima at  $\sim 353$  nm ( $\epsilon = 22800$  M $^{-1}$  cm $^{-1}$ ) and 241 nm ( $\epsilon = 7800$  M $^{-1}$  cm $^{-1}$ ), which have been tentatively assigned as  $\pi$  to  $\pi^*$  transitions.<sup>11,12</sup> Upon photoisomerization, the absorption band at 353 nm exhibits a slight hypsochromic shift and decreases in extinction by nearly 50% while the 241 nm band shows only modest changes in extinction. In the present work the energetics associated with the trans to cis photoisomerization as well as the potential energy surfaces of the mepepy ligand have been investigated using time-resolved photothermal and computational methods in an effort to better characterize the physical properties of this important ligand.

## Materials and Methods

**Synthesis of mepepy.** The *trans*-mepepy ligand was prepared according to the procedure outlined in ref 1 Under an argon atmosphere, 905  $\mu$ L of 4-picoline in 4 mL of anhydrous dimethylformamide (DMF) was added to a suspension of 370 mg of sodium hydride (60% dispersion in mineral oil) in 10 mL of anhydrous DMF. The solution was stirred at 60 °C for 2 h. A solution of 1.01 g of *N*-methylpyrrole-2-carboxyaldehyde in 6 mL of anhydrous DMF was then added to the anion (red solution) and stirred overnight at 60 °C. The solution was poured onto ice and filtered to extract a yellow solid. The filtrate was concentrated and purified with a silica gel column (hexane:ethyl alcohol, 2:1, 1:1, and 1:2). The purity for the compound was verified by NMR spectroscopy.

The quantum yield,  $\Phi$ , associated with the trans  $\rightarrow$  cis isomerization was determined by irradiating a cuvette containing 0.19 mM of mepepy in water with 1% dimethyl sulfoxide (DMSO) with 355 nm radiation (the wavelength used to perform the PAC measurements). The solution was irradiated for a total of 35 min, and the absorption spectra were recorded every 5 min. The same experiment was performed with 0.8 mM azobenzene as a control. The value of  $\Phi$  was then determined using the following equation:

$$\left(\frac{\Delta A_{0-35}^{\text{mep}}}{\Delta A_{0-35}^{\text{azo}}}\right) = \left\{ \left(\Phi^{\text{mep}} \Delta \epsilon^{\text{mep}} C_0^{\text{mep}}\right) / \left(\Phi^{\text{azo}} \Delta \epsilon^{\text{azo}} C_0^{\text{azo}}\right) \right\} \quad (1)$$

where  $\Delta A_{0-35}^{\text{mep}}$  and  $\Delta A_{0-35}^{\text{azo}}$  are the changes in absorbance at 355 nm for mepepy and azobenzene, respectively,  $\Phi^{\text{mep}}$  is the quantum yield for the mepepy trans  $\rightarrow$  cis isomerization,  $\Phi^{\text{azo}}$  is the quantum yield for the trans  $\rightarrow$  cis isomerization associated with azobenzene (0.26),  $\Delta \epsilon^{\text{mep}}$  (2.2 M $^{-1}$  cm $^{-1}$ ) and  $\Delta \epsilon^{\text{azo}}$  (0.4 M $^{-1}$  cm $^{-1}$ ) are the differences in extinction coefficients at 355 nm between the trans and cis forms of mepepy and azobenzene, respectively, and  $C_0^{\text{mep}}$  and  $C_0^{\text{azo}}$  are the initial concentrations. With use of this method,  $\Phi^{\text{mep}}$  was determined to be 0.28.

**Photoacoustic Calorimetry.** The energetics associated with the trans to cis photoisomerization of mepepy were determined using photoacoustic calorimetry (PAC). Photoacoustic calorimetry is proving to be a powerful technique for determining the magnitude and time scale of conformational changes as well as reaction thermodynamics associated with photoinitiated processes.<sup>14</sup> The physical principle behind this method is that photoexcited molecules dissipate excess energy nonradiatively, resulting in thermal heating of the surrounding solvent. In the case of aqueous solutions this causes rapid volume expansion ( $\Delta V_{\text{th}}$ ), resulting in an acoustic wave that can be detected with a sensitive piezoelectric crystal based microphone. In addition, volume changes in the system of interest resulting from conformational/solvation changes associated with a photoinitiated reaction ( $\Delta V_{\text{con}}$ ) also contribute to the acoustic wave. The contributions from  $\Delta V_{\text{th}}$  and  $\Delta V_{\text{con}}$  to the total sample signal,  $S$  (either acoustic amplitude or deflection amplitude) can be evaluated by examining the temperature dependence of the signal and using a calibration compound ( $S_{\text{ref}}$ ) (see ref 14 for theoretical details).

The amplitude of the acoustic wave for the sample mepepy is

$$S_{\text{samp}} = K E_a (\beta / C_p \rho) Q + \Delta V_{\text{con}} \quad (2)$$

where  $S$  is the acoustic wave amplitude,  $K$  is an instrument response parameter,  $E_a$  is the number of einsteins absorbed by the molecule,  $\beta$  is the thermal expansion coefficient of the solvent (K $^{-1}$ ),  $C_p$  is the solvent heat capacity (cal g $^{-1}$  K $^{-1}$ ),  $\rho$  is the solvent density (g mL $^{-1}$ ),  $Q$  is the amount of heat returned to the solvent (kcal mol $^{-1}$ ), and the  $\Delta V_{\text{con}}$  is the nonthermal volume change (mL mol $^{-1}$ ). The corresponding amplitude of the reference acoustic wave is expressed as

$$S_{\text{ref}} = K E_a (\beta / C_p \rho) E_{h\nu} \quad (3)$$

The reference converts the energy of the absorbed photon,  $E_{h\nu}$ , into heat within the excitation pulse width and with a quantum yield of unity (i.e.,  $\Delta V_{\text{con}} = 0$ ). Changes in molar volume and enthalpy are determined by taking a ratio of the acoustic amplitudes of the sample to the reference ( $(S_{\text{samp}}/S_{\text{ref}}) = \phi$ ) as a function of temperature (i.e.,  $C_p$ ,  $\rho$ , and  $\beta$  are all known for different temperatures) according to

$$\phi E_{h\nu} = Q + (C_p \rho / \beta) \Delta V_{\text{con}} \quad (4)$$

The value of  $\Delta V$  is then the slope of eq 4 divided by the quantum yield,  $\Phi$ , of the process being examined. The corresponding enthalpy is determined from

$$\Delta H = (E_{h\nu} - Q) / \Phi \quad (5)$$

For the PAC experiments the *trans*-mepepy ligand was first dissolved in DMSO (mepepy is only slightly soluble in water) to form a stock solution. The PAC sample was then prepared

by addition of mepepy from the stock solution into water to give a final optical density at the excitation wavelength (355 nm) of 0.4 (final [DMSO] was <1% (v/v)). The calorimetric reference used here is iron(3+)tetrakis(4-sulfonatophenyl)porphyrin (Fe4SP), and the reference was prepared as per the mepepy sample (i.e., <1% (v/v) DMSO/water). During all acquisitions, the sample was stirred to minimize photoproduct accumulation. The acoustic traces are the average of five laser pulses. Pulsed laser excitation was accomplished using a Continuum MiniLite I frequency tripled Nd:YAG laser (355 nm, ~7 ns fwhm, ~100  $\mu$ J/pulse, 1 Hz), and the acoustic waves were detected using a Panametrics V103 detector coupled to a Panametrics preamplifier and recorded using a 50 MHz transient digitizer (PicoScope).

**Computational Methods.** Electronic structure calculations of mepepy were performed using the quantum chemistry program GAMESS.<sup>15</sup> Molecular properties were evaluated using density functional theory (DFT) because this has been shown to yield accurate results for isomerization studies of azobenzene, a molecule that is structurally similar to mepepy.<sup>16–18</sup> The B3LYP hybrid exchange-correlation functional was employed for all calculations along with the augmented correlation-consistent double- $\zeta$  basis set (aug-cc-pVDZ).<sup>19–22</sup> Solvation effects were taken into account through the use of a polarizable continuum model in which the mepepy molecule is embedded in an isotropic dielectric field parametrized to mimic the aqueous environment.<sup>23</sup> The dielectric constant was 78.39, and the solvent radius was 1.3850 Å. Geometry optimizations for both the cis and trans isomers were performed in the solvation field in order to ascertain the minimum energy geometries. The molecular electric dipole moments for the optimized structures were determined from the charge distributions. To discover any additional local energy minima, the ground-state cis and trans potential energy surfaces were generated as a function of the angles for the pyridine and pyrrole rings from a planar configuration. Each angle was scanned by rotating the rings along the  $\alpha$ - $\beta$  and  $\gamma$ - $\delta$  vectors, from 0 to 180° in 10° increments, while allowing the remaining degrees of freedom to adopt a minimum conformation. Spectroscopic calculations were performed using ArgusLab<sup>24</sup> using the ZINDO/CI method. The calculations were performed using the highest 45 occupied and lowest 45 unoccupied orbitals in the CI (SCF-CI, restricted Hartree-Fock, with STO-6G minimal basis set). A self-consistent reaction field was also employed with a dielectric constant of 78.3 and a cavity radius of 4.616 Å (SPCE water model).

## Results and Discussion

**Optical Properties.** The steady-state absorption spectrum of the as-isolated trans form of mepepy solubilized in water is displayed in Figure 2. The absorption maximum is observed at ~355 nm with a shoulder centered at ~425 nm. The 355 nm (calculated, 371 nm) band can be assigned primarily from a transition between the HOMO, with electron density centered primarily on the five-membered ring and LUMO orbitals with electron density distributed between the five- and six-membered rings (i.e.,  $\pi$  to  $\pi^*$  transition; see Figure 3). The 425 nm shoulder arises from  $\pi$  to  $\pi^*$  transitions associated with the protonated form of mepepy (i.e., protonation of the pyridine ring nitrogen). This is evident from the disappearance of the ~425 nm band in dilute NaOH solutions (<0.1 M NaOH). Upon steady state illumination of the trans form of mepepy photoisomerizes to the cis form takes place, resulting in a slight hypsochromic shift in the energy of the  $\pi$  to  $\pi^*$  transition for both the protonated

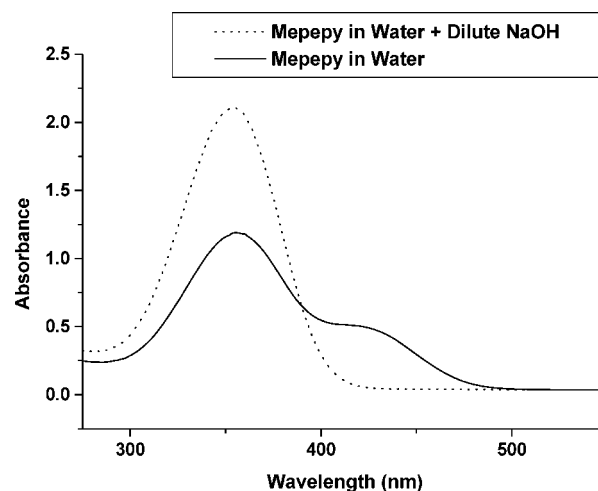


**Figure 2.** Steady-state optical absorption spectra of mepepy in water (containing <1% DMSO) (solid line) and aqueous 0.01 N NaOH (containing <1% DMSO; dotted line). [mepepy] = 270  $\mu$ M.

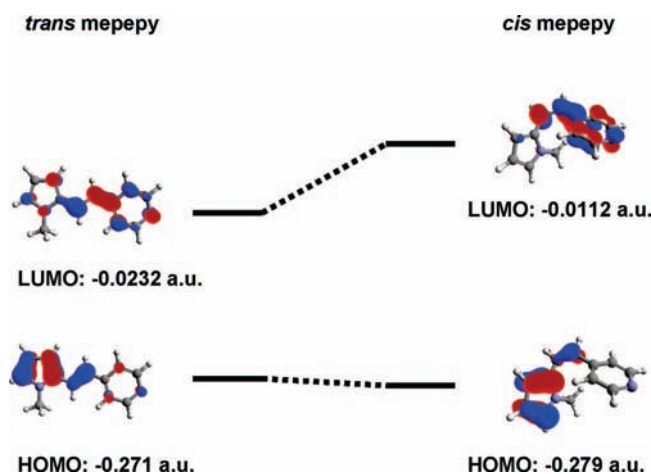


**Figure 3.** Molecular orbital diagrams showing the HOMOs and LUMOs associated with the observed  $\pi$  to  $\pi^*$  transitions of the trans (left) and cis (right) isomers of mepepy.

and deprotonated forms as well as a significant decrease in the molar extinction coefficient (Figure 4). Interestingly, the HOMO of the cis conformer retains significant electron density on the five-membered ring while the LUMO has significant electron density shifted onto the six-membered pyridine ring.

**Theoretical Structural Analysis.** The structures of the energy minima located along the potential energy surface were found (for which the geometric details are tabulated in Tables 1 and 2) and are also visually depicted in the rendered representation of Figures 1, 5, and 6. The energy difference between the global trans minimum and that of the cis form was found to be 8.24 kcal mol<sup>-1</sup>, while the energy difference between the local trans minimum and the cis isomer was determined to be 7.17 kcal mol<sup>-1</sup>. After evaluating the electrostatic moments, the difference in the dipole moment between the global trans state and the cis state was 0.424 D and the local minimum difference was 0.0398 D. While the relative populations of the isomers after a photoisomerization event are unknown, these determined differential values place an upper and lower bound to the true equilibrium differences. The cis potential energy surface is a shallow basin with a single minimum, where it can be expected that the equilibrium structure will fluctuate out of plane in the solvated ground state. However, unique characteristics of the trans potential energy surface were

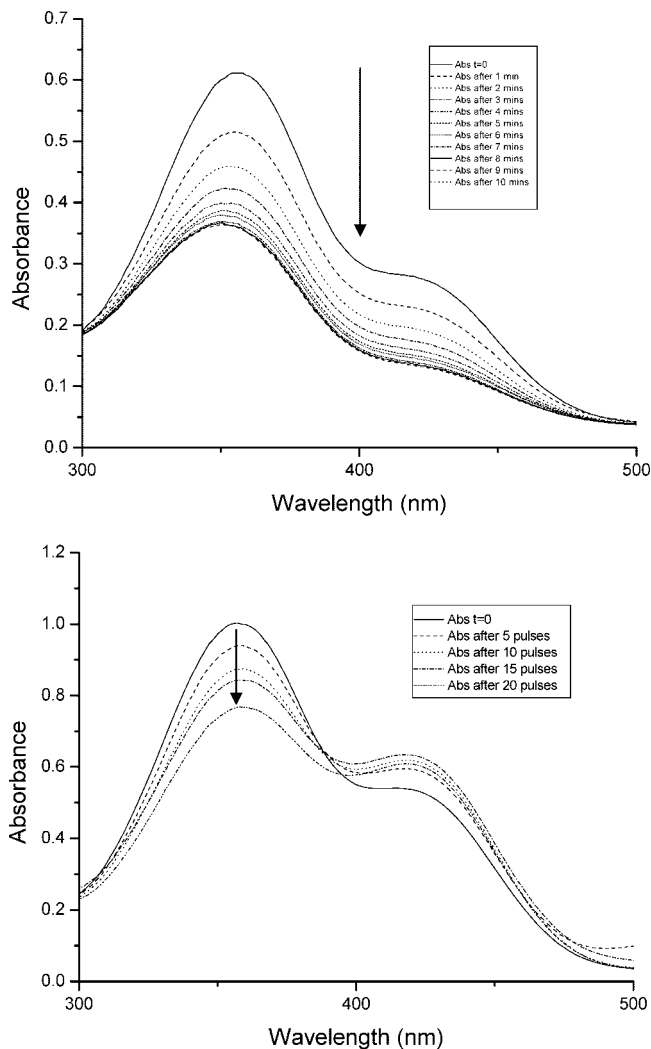


**Figure 4.** Top: Equilibrium UV–vis spectra of mepepy before and after steady-state photolysis (from 10 to 70 min). The sample was solubilized in deionized water containing <1% DMSO. Bottom: Equilibrium UV–vis spectra of *trans*-mepepy before and after 5, 10, 15, and 20 laser pulses ( $\lambda_{\text{excit}} = 355 \text{ nm}$ ,  $\sim 100 \mu\text{J/pulse}$ , and  $\sim 7 \text{ ns}$  fwhm).

**TABLE 1: Geometric Configurations of the Global Energy-Minimized *cis*- and *trans*-mepepy<sup>a</sup>**

	cis isomer		trans isomer	
$\angle\alpha\beta\gamma$ (deg)	126.647	126.490	134.764	135.337
$\angle\beta\gamma\delta$ (deg)	129.507	127.365	144.983	143.931
$d_{\alpha\beta}$ (Å)	1.48689	1.46157	90.0	0.0

<sup>a</sup> The bond angles and distances are with respect to the labels in Figure 1.  $\sigma$  is the angle between the pyridine and pyrrole planes.

**TABLE 2: Calculated Energy and Dipole Moment of Global Minima *cis*- and *trans*-mepepy Isomers, along with the Alternate Local Minimum along the *trans* Potential Energy Surface**

isomer	energy (kcal mol <sup>-1</sup> )	molecular dipole moment (D)
cis	-335330.35	4.12
global trans	-335338.59	3.69
local trans	-335337.51	3.08

found, most notably the existence of two ground-state minima separated by an energy barrier, herein referred to as the global and local *trans* states (geometrically shown in Figure 6).

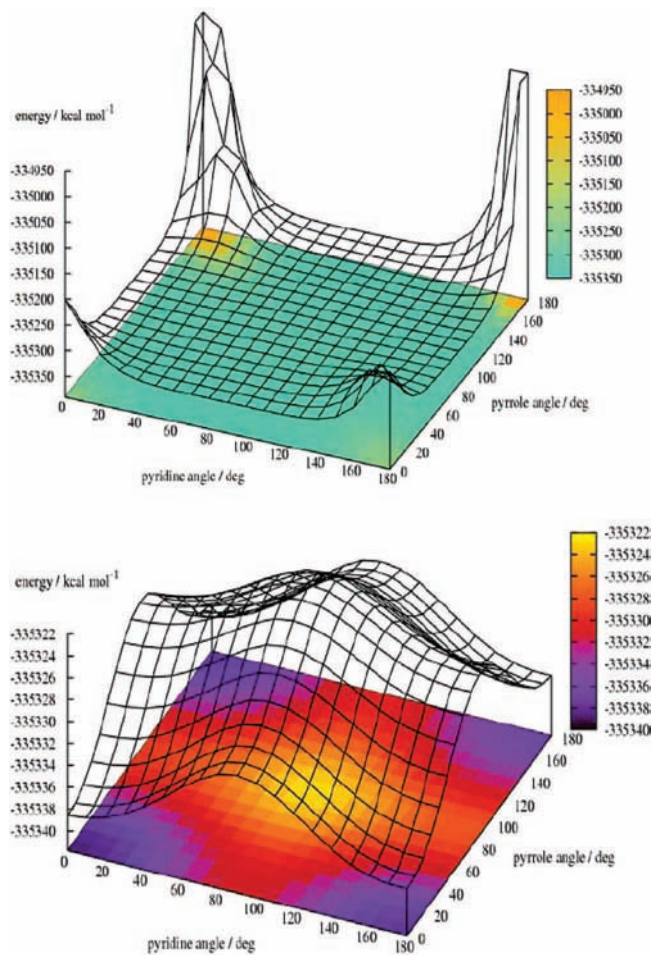


**Figure 5.** *Trans* and *cis* ground-state energy surfaces as a function of the pyridine and pyrrole ring angles as defined by deviation from planar configuration. See text for details.

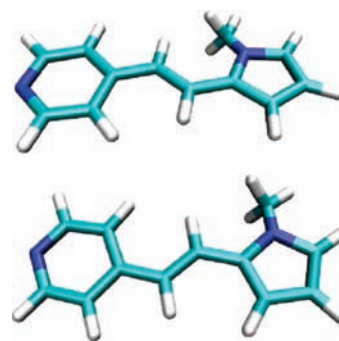


**Figure 6.** Visual rendering of the global and local *trans* geometries (top and bottom, respectively).

Complete determination of the isomerization mechanism for mepepy (which is not determined in this work) is required to know whether the transitions from the excited state to the ground state favor one isomeric *trans* form over the other. The minimum energy barrier between the cogeneric *trans* states is 9.12 kcal mol<sup>-1</sup>, whereas the thermal energy  $kT$  at 300 K is only 0.596 kcal mol<sup>-1</sup>.

**Photothermal Studies.** Figure 7 displays overlays of the PAC signals for mepepy and the Fe4SP reference compound at 35 °C. The photoacoustic signals for the mepepy *trans* to *cis* isomerization do not show any shift in frequency, relative to the calorimetric reference, indicating that the  $\Delta H$  and  $\Delta V$  occur within the response time of the PAC instrument, i.e.,  $< \sim 50 \text{ ns}$ .

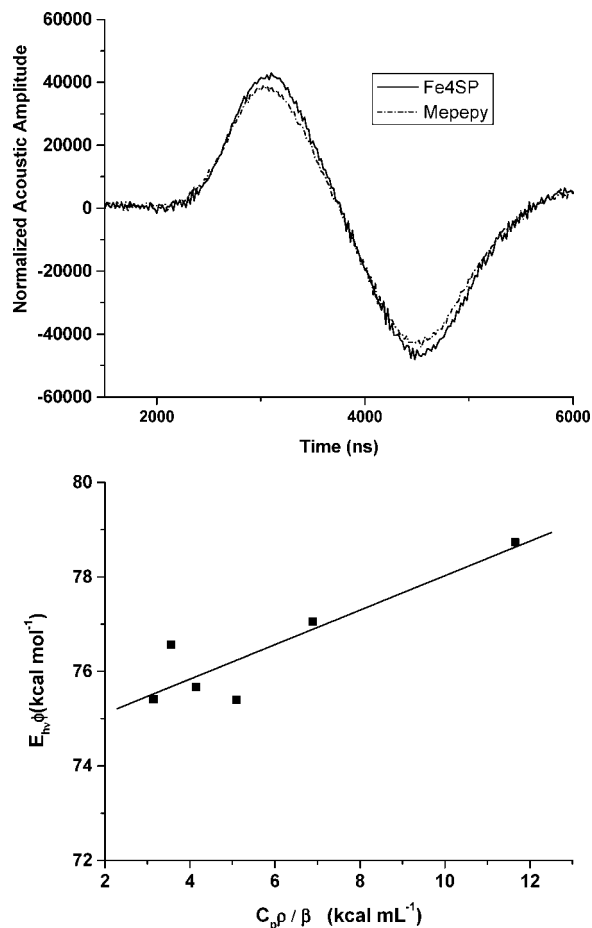


**Figure 7.** Overlay of the normalized acoustic wave of the reference Fe4SP and the *trans*-mepepy at 35 °C. The absorbance of the sample and reference at the excitation wavelength (355 nm) was 0.4. Both the sample and reference signals were obtained in water containing <1% DMSO.

From a plot of  $\phi E_{hv}$  versus  $(C_p \rho / \beta)$  the volume and enthalpy changes are determined to be  $\Delta V = 0.9 \pm 0.4$  mL mol<sup>-1</sup> and a  $\Delta H = 18 \pm 3$  kcal mol<sup>-1</sup> (see Figure 8 for volume and enthalpy profiles).

Two key factors influence the magnitude of the molar volume change: (1) changes in van der Waals volume of the mepepy molecule itself upon isomerization and (2) subsequent changes in solvent structure surrounding the chromophore due to changes in the ground-state dipole moment and/or changes in the overall charge on the molecules. The volume change due to electrostriction can be estimated using

$$\Delta V_{el} = -(\mu^2/r^3)\kappa_T\{(\epsilon + 2)(\epsilon - 1)/(2\epsilon + 1)^2\}(N_A/4\pi\epsilon_0) \quad (6)$$

where  $\mu$  is the dipole moment,  $r$  is the cavity radius of the molecule,  $\kappa_T$  is the compressibility of the solvent,  $\epsilon$  is the solvent's dielectric constant,  $N_A$  is Avogadro's number, and  $\epsilon_0$  is the vacuum permittivity.<sup>25,26</sup> Using the calculated dipole change for the *trans* to *cis* isomerization of 0.0398 D, a molecular radius of  $\sim 5$  Å (this assuming the mepepy molecule sweeps out a sphere of diameter  $\sim 10$  Å),  $\kappa_T$  of  $4.22 \times 10^{-10}$  Pa<sup>-1</sup> (for water at 25 °C) and  $\epsilon = 78.4$ , the volume change due to electrostriction is estimated to be  $\sim -0.2$  mL mol<sup>-1</sup>. The corresponding change in van der Waals volumes between the *trans* and *cis* isomers are estimated to be  $\sim 9$  mL mol<sup>-1</sup> with the *cis* conformation having the lower molar volume. Thus,  $\Delta V$

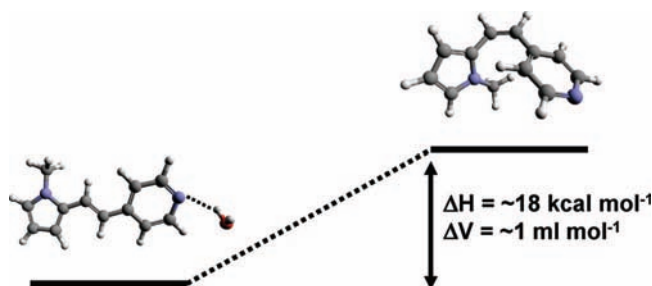


**Figure 8.** Thermodynamic profile for the photoinduced *trans* → *cis* isomerization of mepepy in aqueous solution.

would be expected to be on the order of  $\sim -9.2$  mL mol<sup>-1</sup>. This value is significantly lower than the observed  $\Delta V = \sim 0.9$  mL mol<sup>-1</sup>, indicating that solvent–mepepy interactions are distinct between the *trans* and *cis* conformations. Examination of the HOMO orbitals for the *cis* and *trans* conformations (as discussed above) reveals less electron density on the pyridine N-atom in the *cis* conformer relative to the *trans* conformer which is expected to reduce the extent of H-bonding between a water molecule and the mepepy pyridine group. In fact, bond cleavage reactions typically result in an average increase in molar volume of  $\sim +5$  mL mol<sup>-1</sup>.<sup>27</sup> Thus, the  $\Delta V$  value obtained from PAC would be consistent with a loss in H-bonding in the *cis* conformer relative to the *trans* conformer with the  $\Delta V^{H-bond} \sim +9$  mL mol<sup>-1</sup>.

The corresponding change in enthalpy, obtained from the PAC results, is 18 kcal mol<sup>-1</sup>. In contrast, the results of the computational studies suggest an energy difference of only  $\sim 8$  kcal mol<sup>-1</sup> between the global energy minima between the *cis* and *trans* conformers. The  $\sim 10$  kcal mol<sup>-1</sup> difference in energies must also be due to distinct interactions between the mepepy conformers and the aqueous solvent. Previous studies of hydrogen bonding interactions between water and pyridine have shown that the hydrogen bond energy on the order of 6–8 kcal mol<sup>-1</sup>, very near the difference observed between the theoretical energy difference and that observed from PAC.<sup>28–30</sup> Thus, the change in enthalpy between the *cis* and *trans* conformers is also consistent with the loss of a hydrogen bond between water and the pyridine N subsequent to the isomerization.

In summary the results presented here demonstrate several key features of the *trans* to *cis* conversion in mepepy. First, the mepepy ligand exhibits two conformational minima for the *trans* state that are separated by 9 kcal mol<sup>-1</sup>, suggesting that the photoinduced spin-state transitions associated with metal complexes containing the mepepy ligand may be energetically “tuned” on the basis of the nature of the *trans* conformer. Second, the results of the computational studies reveal very little change in dipole moment between the *trans* and *cis* conformers of mepepy, indicating more subtle changes in the electronic structure of mepepy relative to other push–pull molecules and the azobenzenes. Finally, the results of the PAC studies suggest that the thermodynamics associated with the *trans* to *cis* isomerization can be modulated by the nature of the solvent. Solvents which hydrogen bond with the N-atom of the mepepy pyridine group can stabilize the *trans* conformation by up to 10 kcal mol<sup>-1</sup>.

**Acknowledgment.** The authors acknowledge the Petroleum Research Fund (ACS-PRF43423-AC4) for support for this work.

## References and Notes

- (1) Bradamante, S.; Facchetti, A.; Pagani, G. A. *J. Phys. Org. Chem.* **1997**, *10*, 514.

- (2) Isaksson, G.; Sandstrom, J. *Acta Chim. Scand.* **1973**, *27*, 1183.
- (3) Chemla, D. S.; Zyss, J., Eds. *Non-Linear Optical Properties of Organic Molecules and Crystals*, Vols. 1 and 2; Academic Press: New York, 1986.
- (4) Cheng, L. T.; Tam, W.; Stevenson, S. H.; Meredith, G. R.; Rikken, G.; Marder, S. R. *J. Phys. Chem.* **1991**, *95*, 10631.
- (5) Oudar, J. L. *J. Chem. Phys.* **1977**, *67*, 446.
- (6) Prasad, P. N.; Williams, D. J. *Introduction to Nonlinear Optical Effects in Molecules and Polymers*; John Wiley and Sons: New York, 1994.
- (7) Quenneville, J.; Martinez, T. J. *J. Phys. Chem.* **2003**, *107*, 829.
- (8) Zarebowitch, J.; Roux, C.; Boillot, M.-L.; Claude, R.; Itie, J.-P.; Polian, A.; Bolte, M. *Mol. Cryst. Liq. Cryst.* **1993**, *234*, 247.
- (9) Decurtis, S.; Gutlich, P.; Kohler, C. P.; Spiering, H.; Hauser, A. *Chem. Phys. Lett.* **1984**, *105*, 1.
- (10) Boillot, M.-L.; Roux, C.; Audiere, J.-P.; Dausse, A.; Zarebowitch, J. *Inorg. Chem.* **1996**, *35*, 3975.
- (11) Sour, A.; Boillet, M.-L.; Riviere, E.; Lesot, P. *Eur. J. Inorg. Chem.* **1999**, 2117.
- (12) Boillot, M.-L.; Chantraine, S.; Zarebowitch, J.; Lallemand, J.-Y.; Prunet, J. *New J. Chem.* **1999**, 179.
- (13) Faulmann, C.; Dorbes, S.; Garreau de Bonneval, B.; Molnar, G.; Bousseksou, A.; Gomez-Garcia, C. J.; Coronado, E.; Valade, L. *Eur. J. Inorg. Chem.* **2005**, 3261.
- (14) Larsen, R. W.; Miksovska, J. *Coord. Chem. Rev.* **2007**, *251*, 1101.
- (15) Schmidt, M. W.; Baldrige, K. K.; Boatz, J. A.; Elbert, S. T.; Gordon, M. S.; Jensen, J. H.; Koseki, S.; Matsunaga, N.; Nguyen, K. A.; Su, S.; et al. *J. Comput. Chem.* **1993**, *14*, 1347.
- (16) Crecca, C. R.; Roitberg, A. E. *J. Phys. Chem.* **2006**, *110*, 8188.
- (17) Cembran, A.; Bernardi, F.; Garavelli, M.; Gagliardi, L.; Orlandi, G. *J. Am. Chem. Soc.* **2004**, *126*, 3234.
- (18) Tiago, M. L.; Ismail-Beigi, S.; Louie, S. G. *J. Chem. Phys.* **2005**, *122*, 94311.
- (19) Becke, A. D. *J. Chem. Phys.* **1993**, *98*, 5648.
- (20) Stephens, P.; Devlin, F.; Chabalowski, C.; Frisch, M. J. *J. Phys. Chem.* **1994**, *98*, 11623.
- (21) Hertwig, R.; Koch, W. *Chem. Phys. Lett.* **1997**, *286*, 345.
- (22) Dunning, T. H. *J. Chem. Phys.* **1989**, *90*, 1007.
- (23) Semiati, R.; Leshinski, E.; Orell, A.; Cossi, M.; Barone, V.; Cammi, R.; Tomasi, J. *J. Chem. Phys. Lett.* **1996**, *255*, 327.
- (24) *ArgusLab 4.0*; Mark A. Thompson, Planaria Software LLC: Seattle, WA, 2008, <http://www.ArgusLab.com>.
- (25) Padova, J. *J. Chem. Phys.* **1963**, *39*, 1552.
- (26) Wegewijs, B.; Paddon-Row, M. N.; Braslavsky, S. E. *J. Phys. Chem. A* **1998**, *102*, 8812.
- (27) van Eldik, R.; Asano, A.; le Noble, W. J. *Chem. Rev.* **1989**, *89*, 549.
- (28) Papai, I.; Jansco, G. *J. Phys. Chem. A* **2000**, *104*, 2132.
- (29) Zega, A.; Srcic, S.; Mavri, J.; Bester-Rogac, M. *J. Mol. Struct.* **2008**, *875*, 354.
- (30) Marczyk, W.; Lejmann, J. K.; Heintz, A. *J. Chem. Therm.* **2003**, *35*, 269.

JP803268R